

PAPER

## Chaotic Resonance in Forced Chua's Oscillators

Kazuyoshi Ishimura, Tetsuya Asai and Masato Motomura

Graduate School of Information Science and Technology, Hokkaido University

Kita 14, Nishi 9, Kita-ku, Sapporo 060-0814, Japan

E-mail: ishimura@lalsie.ist.hokudai.ac.jp, {asai, motomura}@ist.hokudai.ac.jp

**Abstract** Stochastic resonance (SR) is a phenomenon in which dynamic noise is effectively used to induce state transitions in a double-well potential system driven by subthreshold input signals. The noises are supplied to the system as an additional force. Recently, a phenomenon called “chaotic resonance” (CR) has been spotlighted in the literature. CR can be observed in chaotic systems that have multiple strange attractors and the ability to accept subthreshold input signals; *i.e.*, such CR systems do not require any external noise source, unlike traditional SR systems. In this study, we employed Chua's oscillator as a candidate CR system. The oscillator was driven by a sinusoidal voltage source providing subthreshold input signals. In a certain range of input signal frequencies, we observed chaotic state transitions between the two attractors, whereas no state transition between the attractors was observed in the remaining frequency range. These findings indicated that chaotic fluctuations assisted the state transition. Furthermore, we observed nonmonotonic CR characteristics (correlation value and signal-to-noise ratio between the input signal and the output signal) that corresponded to typical nonmonotonic SR curves.

**Keywords:** stochastic resonance, chaotic resonance, Chua's oscillator

### 1. Introduction

Noises in electronic circuits, particularly those in analog circuits, have adverse effects on the desired circuit operations [1]. Therefore, extensive research has been conducted to devise electronic circuits that reduce these noises. On the other hand, many biological systems process information with the help of external or thermal noises, for example, see [2–10]. To reproduce this behavior, circuits that exploit noises efficiently, instead of removing them, have been proposed [11–17].

Among various strategies of exploiting noises in nature, *stochastic resonance* (SR) is believed to be a fundamental phenomenon in which external noise is effectively used. Indeed, biological systems effectively utilize the noise generated by their own dynamics to invoke SR, and this mechanism has previously been investigated [18, 19]. Among such SR driven by self-generated noises, *chaotic resonance* (CR) has been spotlighted in the literature [20–24]. CR is a phenomenon in which internal fluctuations are effectively used to trigger state transitions; therefore, CR does not require external noise. Furthermore, CR may play an important role in cerebellar learning [25], and thus, one can postulate that biological systems tend to use external and internal fluctuations.

In this study, we attempted to determine simpler CR systems by focusing on the chaotic systems that produce internal fluctuations. We here assumed that our CR could be observed in chaotic systems that satisfy the following condi-

tions: (i) the system must contain two strange attractors that corresponded to the system states and (ii) the system's state transition must be caused by external input signals. Condition (i) is necessary for mimicking the two states of conventional SR in double-well (bistable) systems. Regarding condition (ii), we considered that under certain parameter conditions with a subthreshold input signal, the state transitions would not be induced (the state would be trapped in one of the attractors), and the state transition would occur when the amount of chaotic fluctuations generated internally exceeds a certain threshold (the state would pass through the attractors). Duffing, Lorenz, and double-scroll systems are a few of such chaotic systems. Lorenz and double-scroll systems are autonomous and can cause chaotic state transitions without an input signal. Among the many double-scroll chaotic systems, Chua's oscillator [26] is known to be suitable for choosing a parameter set that satisfies the above-mentioned conditions (i and ii) that must be met for state trapping and transition. Hence, we employed Chua's oscillator as a candidate CR system.

To elucidate the relationship between the degree of CR and the strength of the fluctuation generated by Chua's oscillator, we evaluate the correlation value and SNR between the input signal and the output signal, as in evaluations of conventional SR systems, and show that the characteristics of the correlation value and SNR may correspond to typical SR curves. Furthermore, since arrayed threshold units are known to en-

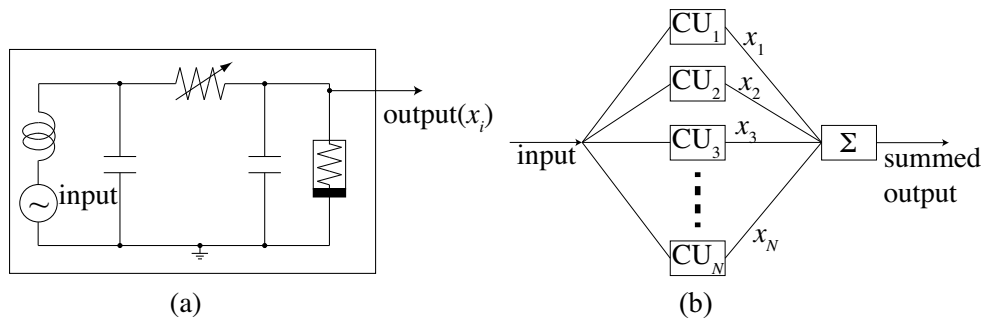


Fig. 1 (a) Chua's oscillator unit (CU), and (b) Summing network of Chua's oscillators (CU) with common input and summed output signals

hance the correlation value for a wide range of noise intensity levels in SR [19,27], we evaluate a network that consists of arrayed Chua's oscillators, and show that the network enhances the correlation values.

This paper is organized as follows. Section 2 describes the simulation methods and setups. The results for single and arrayed Chua's oscillators are presented in Sect. 3. Section 4 is devoted to the summary and discussion.

## 2. Methods

In this research, we applied a sinusoidal voltage as an input signal to Chua's oscillator, which consists of five electrical elements (a resistor, two capacitors, an inductor, and a nonlinear resistance), as shown in Fig. 1(a). Despite its simple structure, this oscillator exhibits a wide variety of chaotic phenomena and bifurcations, and has two attractors. We here define the system's state as the trapped region among the attractors. The dynamics of the forced Chua's oscillator can be written as follows:

$$\begin{aligned}\dot{x} &= c_1(y - x - g(x)) \\ \dot{y} &= c_2(x - y + z) \\ \dot{z} &= -c_3y + A \sin(2\pi ft)\end{aligned}$$

where  $A \sin(2\pi ft)$  represents the input signal ( $A$ : amplitude,  $f$ : frequency),  $c_{1,2,3}$  represents the system parameters, and  $g(x)$  represents the normalized nonlinear resistance, which is given by

$$g(x) = m_0x + \frac{1}{2}(m_1 - m_0)|x + B_P| + \frac{1}{2}(m_0 - m_1)|x - B_P|$$

where  $m_{0,1}$  and  $B_P$  represent the resistance parameters.

To induce the state transitions between the attractors, we set the Chua's oscillator parameters to values such that no state transition occurs without the input signal, and then set

the input signal amplitude ( $A$ ) to a subthreshold value near the threshold value. Then, we varied the input signal frequency ( $f$ ) as the Chua's oscillator parameter. Under these conditions, the state transitions can be presumed to have been assisted by not the input signal amplitude but the chaotic fluctuations generated by Chua's oscillator.

Furthermore, we considered a network consisting of an array of Chua's oscillators and investigated whether using the network would enhance the correlation value and SNR in CR. A common subthreshold input signal was supplied to an array of Chua's oscillators. Then, output signals of the array of Chua's oscillators ( $x_1 \dots x_N$ ) were summed, as illustrated in Fig. 1(b).

## 3. Results

### 3.1 Attractor trapping and transition with input signal

We set the parameters of Chua's oscillator as  $c_1 = 15.6$ ,  $c_2 = 1$ ,  $c_3 = 33$ ,  $B_P = 1$ ,  $m_0 = -8/7$ , and  $m_1 = -5/7$ . The input signal amplitude ( $A$ ) was fixed at 2.7, which was insufficient to cause state transitions between the two attractors. Subsequently, we varied the frequency ( $f$ ) of the input signal, considering it to be the system parameter. Figure 2 shows plots of the simulation results for a single Chua's oscillator with  $f = 0.01$  (left to middle in Fig. 2) and 0.15 (right). Figures 2(a), 2(b), and 2(c) show the trajectories of the system variables ( $x$  and  $y$ ). The time course of the Chua's oscillator variable for the output signal ( $x$ ) and the input signal ( $A \sin(2\pi ft)$ ) are plotted in Figs. 2(d), 2(e), and 2(f). When  $f = 0.01$ ,  $x$  does not follow the input signal and the state is trapped in the left or right attractor depending on the initial state value, as shown in Figs. 2(a), 2(b), 2(d), and 2(e). In contrast, when  $f = 0.15$ , the state chaotically transits through the two attractors, as shown in Figs. 2(c) and 2(f).

Figures 2(g), 2(h), and 2(i) show plots of the time course of correlation values between the input signal and  $x$  given by

$$\text{correlation value} =$$

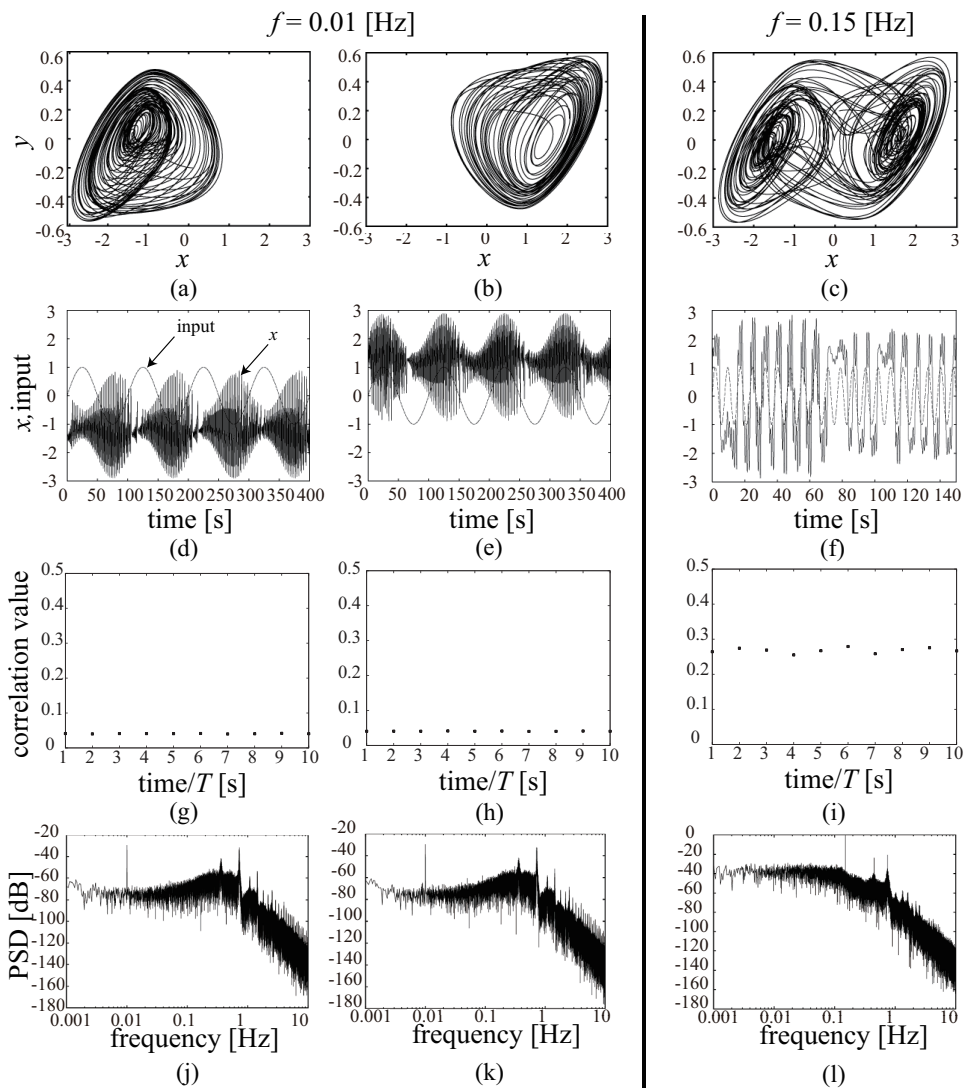


Fig. 2 Simulation results of Chua's oscillator with subthreshold input signal ( $A \sin(2\pi ft)$ ): Phase-plane (a, b, c), Time-series of  $x$  and input signal (d, e, f), Correlation value (g, h, i), and PSD (j, k, l) ( $f = 0.01$  Hz (a, b, d, e, g, h, j, k),  $f = 0.15$  Hz (c, f, i, l), ( $c_1 = 15.6, c_2 = 1, c_3 = 33, B_P = 1, m_0 = -8/7, m_1 = -5/7,$  and  $A = 2.7$ ))

$$\frac{\langle A \sin(2\pi ft) \cdot x(t) \rangle - \langle A \sin(2\pi ft) \rangle \langle x(t) \rangle}{\sqrt{\langle A \sin(2\pi ft)^2 \rangle - \langle A \sin(2\pi ft) \rangle^2} \sqrt{\langle x(t)^2 \rangle - \langle x(t) \rangle^2}}$$

$$\langle X(t) \rangle \equiv \frac{1}{T} \int_{t-T}^t X(t) dt$$

where we set  $T$  at 10000. In Fig. 2(f), we can observe that  $x$  follows the input signal stochastically. When  $f = 0.01$ , correlation values are very low, as shown in Figs. 2(g) and 2(h). On the other hand, when  $f = 0.15$ , the correlation value increased, and the average is around 0.25, as shown in Fig. 2(i).

Figures 2(j), 2(k), and 2(l) show plots of the power spectrum density (PSD)  $X(f)$  obtained by the Fourier transform of  $x(t)$  and then raising it to the second power as follows.

$$X(f) = \frac{1}{2\pi} \left| \int_{-\infty}^{+\infty} x(t) e^{-j2\pi ft} dt \right|^2$$

On this occasion, we sampled  $x(t)$  with the same number of samples and the same time steps among the simulation datasets. Therefore, one may compare the PSD values absolutely among the datasets.

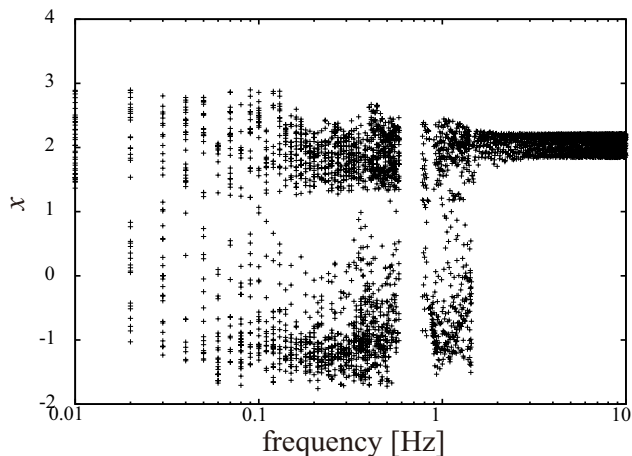


Fig. 3 Bifurcation diagram of  $x$  in Chua's oscillator

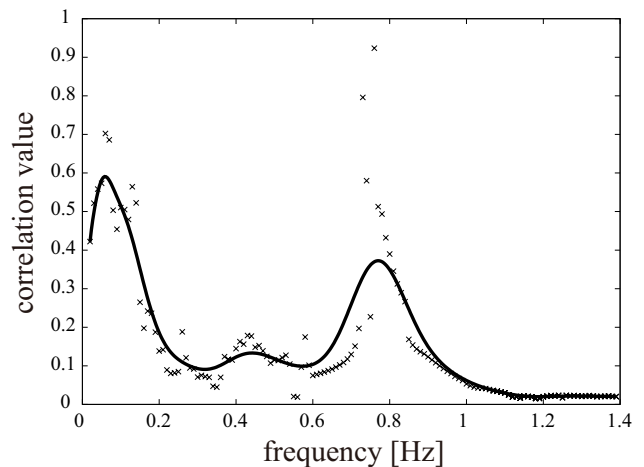


Fig. 4 Correlation value versus the input frequency for Chua's oscillator

The SNR values at the driven frequency  $f_0$  are given by

$$\text{SNR} = 10 \log_{10} \left( \frac{S(f_0)}{B(f_0)} \right)$$

where  $S$  and  $B$  represent the output PSD of the peak and the background level, respectively. The calculated SNR for Figures 2(j), 2(k), and 2(l) were 48 [dB], 47 [dB], and 52 [dB], respectively, and were not so different among the three cases. On the other hand, absolute PSD values in the low-frequency range (lower than  $f_0$ ) were significantly different between the cases shown in Figs. 2(j) and 2(k), and Fig. 2(l), which implies that the increased low-frequency background noise induced the chaotic state transition. The quantitative evaluation is presented in the following section.

### 3.2 Evaluation of degree of chaotic resonance

In the previous subsection, Fig. 2 showed the different behaviors of the Chua's oscillator upon changing the two input signal frequencies (0.01 and 0.15 Hz). Here we sweep the input signal frequency, and show the bifurcation diagram and correlation values in terms of the frequency.

To obtain a bifurcation diagram in Chua's oscillator, we swept the input frequency from 0.01 Hz to 10 Hz in steps of 0.01. In Fig. 3, the  $x$ -axis is the input signal frequency and the  $y$ -axis represents the set of  $x$  values over the simulation time. Figure 3 shows that chaotic transitions occur in the range from 0.02 Hz to 1.2 Hz. In the range from 0.6 Hz to 0.9 Hz,  $x$  was trapped to the power supply voltage. We further investigated the relationship between the input signal frequency and the correlation value, as shown in Fig. 4. From Figs. 3 and 4, we could not find any SR-like relationship between the input signal frequency and  $x$ , or between the input signal frequency and the correlation value. In Chua's oscillator, noise power is determined by the frequency, and then, the

degree of transitions is changed. Hence we investigated the relationship between the degree of resonance in CR and the strength of the fluctuation generated by Chua's oscillator.

In SR, since there is a noise source outside the SR system, the noise density can be controlled and be simply defined as the noise quantity. In contrast, in CR, isolating chaotic fluctuations produced in the system is difficult. We could obtain the chaotic fluctuation power from the output signal combined with an input signal and chaotic fluctuations. The area under the PSD of the output signal is equal to the total signal power with chaotic fluctuations. The proportion of the input signal power is low in the total signal power and ignorable when we calculate chaotic fluctuations power. Therefore, for the sake of simplicity, we considered the output signal power as the noise quantity. The signal power was calculated by integrating the PSD  $X(f)$  from 0.01 Hz to 50 Hz as follows.

$$\text{signal power} = \int_{0.01}^{50} X(f) df$$

Figure 5 shows the correlation value versus the signal power. The correlation value first increases with the noise power, peaks, and then finally decreases. We could identify which characteristics of CR correspond to typical SR curves, as shown in Fig. 5. Optimized internal fluctuations generated by the chaotic system were found to enhance the correlation value in the CR system.

Figure 6 shows the signal intensity dependence of CR characteristics in Chua's oscillator where the  $x$ -axis represents the signal power, the  $y$ -axis the signal input amplifier  $A$ , and the  $z$ -axis the correlation value. The input amplitude ( $A$ ) was changed from 0.3 to 3.0 in steps of 0.3. When  $A$  is small, the correlation value is low because no transition occurs. When transitions occur, the characteristics between the signal power

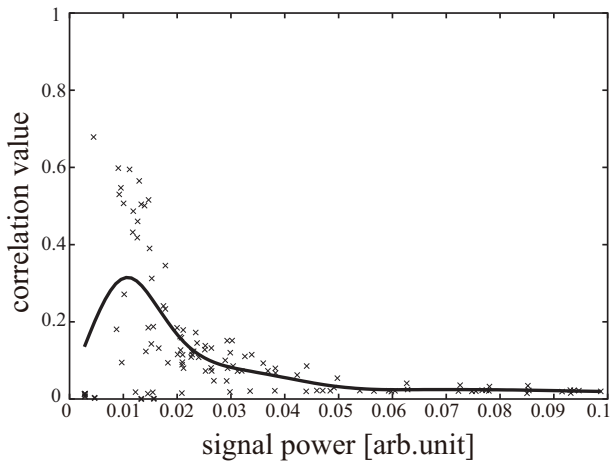


Fig. 5 Correlation value versus signal power for Chua's oscillator

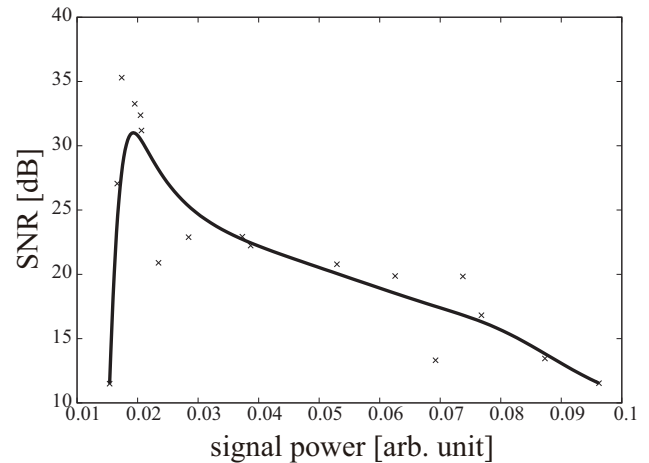


Fig. 7 SNR versus signal power for Chua's oscillator

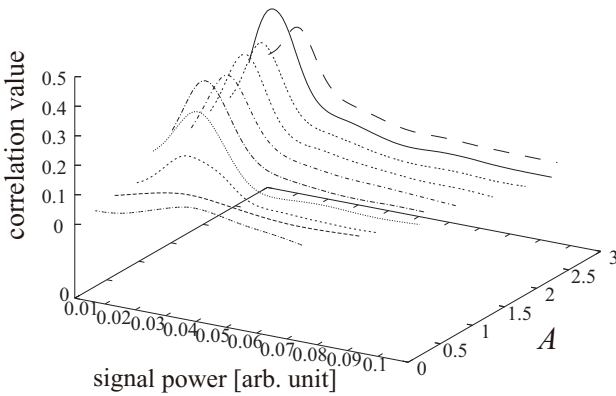


Fig. 6 Signal intensity dependence on CR characteristics of Chua's oscillator

versus the correlation value may have a peak, as expected from Fig. 5. When  $A$  is 2.7, the correlation value peak becomes maximum. Therefore, here, we can conclude that the optimized signal power (noise power) assists frequent transitions.

Next, we calculated the SNR of Chua's oscillator. For this purpose, the output signal  $x$  was converted to a binary signal (1 or  $-1$ ) by applying a threshold function. When the state was trapped in either attractor, the SNR could not be calculated. We could obtain the SNR when the state transitioned between the two attractors. Furthermore, when  $x$  followed the input signal closely, the SNR increased, and when  $x$  weakly followed the input signal, the SNR decreased, as shown in Fig. 7. We determined which SNR characteristics resembled those in the case of typical SR curves by using Fig. 5. These characteristics quantitatively indicated that chaotic fluctuations in the system induced state transitions for a given sub-

threshold input signal, in the same way as SR.

### 3.3 Arrayed Chua's oscillators' network

CR achieved with Chua's oscillator was discussed in the previous sections. We consider an array of Chua's oscillators in this subsection [Fig. 1(b)]. In the network, we computed the correlation value and SNR between the input signal and  $x_{\text{mean}}$ , which is the total output averaged by the number of Chua's oscillators ( $N$ ). The network's signal power was calculated by determining  $x_{\text{mean}}$  and then by integrating this PSD from 0.01 Hz to 50 Hz.

Figure 8 shows the correlation value versus the signal power characteristics for numbers of Chua's oscillators ( $N$ ) of 1, 2, and 10. When the output signals ( $x_1 \dots x_N$ ) were summed to compute the signal power, chaotic fluctuations overlapping the output signals were found to be canceled. Therefore, when  $N$  increased, the maximum correlation value moved to a lower signal-power area. Although Fig. 8 shows apparently different results for arrayed excitable units for SR, we expect that increasing the number of arrayed oscillators would enhance the correlation value. This is because, by increasing the number of oscillators, the distribution of the low correlation value moves to a high-correlation-value area and the signal power decreases, as previously noted.

Figure 9 shows the SNR versus the signal power characteristics for numbers of oscillators ( $N$ ) of 1, 2, and 10. To calculate the SNR in this case, output signals were separately digitized (1 or  $-1$ ) by applying a threshold function and the binary signals were summed. The SNR peak also moved to the lower signal-power area, and the SNR decreased in the high noise-power area ( $N = 1, 2, 10$ ). From Fig. 9, we can expect that increasing the number of Chua's oscillators will enhance the correlation value, as in the case shown in Fig. 8. From these results, we conclude that using the network en-



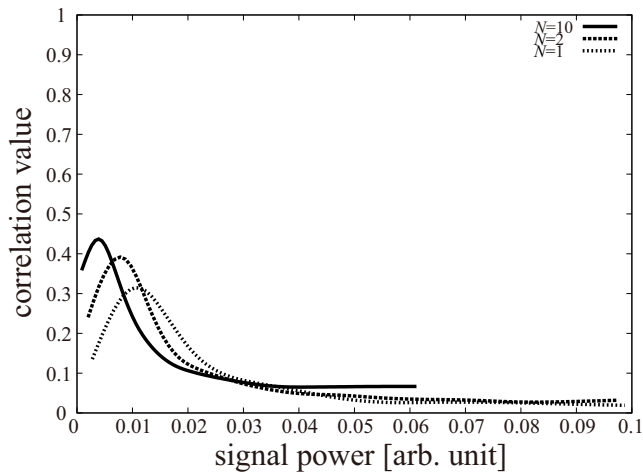


Fig. 8 Correlation value versus signal power for arrayed Chua's oscillator network ( $N = 1, 2, 10$ )

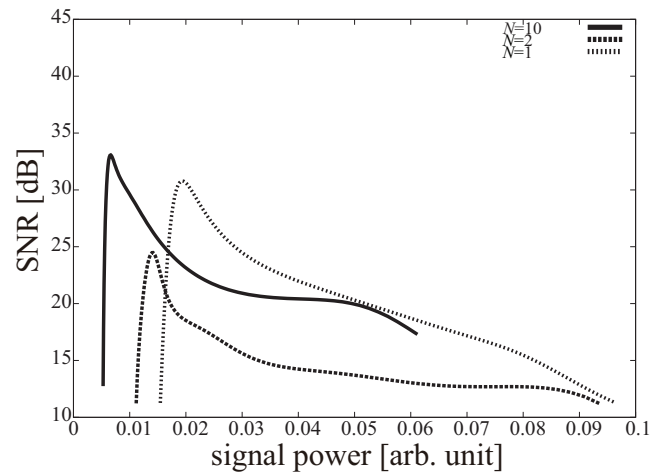


Fig. 9 SNR versus signal power for arrayed Chua's oscillator network ( $N = 1, 2, 10$ )

hances the correlation value and SNR in a CR system.

#### 4. Summary and Discussion

In this study, we observed CR in Chua's oscillator with a subthreshold input signal. We swept the frequency of the input signal in order to observe the oscillator operations. In certain ranges, the Chua's oscillator output signal followed the input signal, and in others, it did not. We investigated the relationship between the degree of resonance and the chaotic fluctuations.

In SR, the external noise density is controlled directly as the noise quantity. For example, in [3], external noise was presented to a crayfish and controlled directly. On the other hand, defining internal noise is difficult because it is cumbersome to extract and control internal noise intensity directly in SR and CR systems. In [18, 19], the coupling strength was defined as the noise quantity. Hence, in this study, we defined the output signal power including internal fluctuations as the noise quantity.

We found the characteristics of the correlation value and SNR, in the case of CR curves, to be similar to typical SR curves. Furthermore, we evaluated the correlation value and SNR for a network consisting of an array of Chua's oscillators having a common input signal and  $x_{\text{mean}}$ . When the number of arrayed Chua's oscillators was increased, the distribution of the SNR and correlation value moved to a region of higher values and the signal power decreased. From these results, we found that using the network enhanced the correlation value and SNR in a CR system. We also found that internal chaotic fluctuations or noise can induce state transitions or help detect a subthreshold input signal, similar to typical SR systems.

Finally we discuss some electrical engineering applications

that use CR. CR in a bistable system, such as the Chua's oscillator that was used in this study, can be used to implement dynamical memory. When the input signal is sufficiently large, the memory operates normally. In the scenario of continuous power-voltage reduction, conventional memories such as SRAM cannot operate in the circuit state correctly, since the input signal has a subthreshold amplitude. However, in the same situation, dynamical memory can overcome this problem and memorize data stochastically by utilizing the chaotic fluctuation effectively, as suggested by the results. Therefore, we can assume that a dynamical memory with CR can achieve low power consumption. Furthermore, CR that uses the chaotic fluctuation examined in this study can utilize another type of noise, for example, quantum noise, which is unavoidable noise that occurs in nanoscale devices. Hence, dynamical memories with CR are a good candidate for use in low-voltage memory, nanoscale memory, and other such devices.

#### References

- [1] D. Abbott: Overview: Unsolved problems of noise and fluctuations, *Chaos*, Vol. 11, No. 3, pp. 526-538, 2008.
- [2] T. Shimozawa and M. Kanou: The aerodynamics and sensory physiology of range fractionation in the cercal filiform sensilla of the cricket *Gryllus bimaculatus*, *J. Comp. Physiol. A*, Vol. 155, No. 4, pp. 495-505, 1984.
- [3] J. K. Douglass, L. Wilkens, E. Pantazelou and F. Moss: Noise enhancement of information transfer in crayfish mechanoreceptors by stochastic resonance, *Nature*, Vol. 365, No. 23, pp. 337-340, 1993.

- [4] D. J. Mar, C. C. Chow, W. Gerstner, R. W. Adams and J. J. Collins: Noise shaping in populations of coupled model neurons, *Neurobiol.*, Vol. 96, No. 18, pp. 10450-10455, 1999.
- [5] T. Mori and S. Kai: Noise-induced entrainment and stochastic resonance in human brain waves, *Phys. Rev. Lett.*, Vol. 88, No. 21, pp. 218101-218104, 2002.
- [6] M. C. W. van Rossum, B. J. O'Brien and R. G. Smith: Effects of noise on the spike timing precision of retinal ganglion cells, *J. Neurophysiol.*, Vol. 89, No. 5, pp. 2406-2419, 2003.
- [7] K. Funke, N. J. Kerscher and F. Wörgötter: Noise-improved signal detection in cat primary visual cortex via a well-balanced stochastic resonance like procedure, *Eur. J. Neurosci.*, Vol. 26, No. 5, pp. 1322-1332, 2007.
- [8] T. M. Hospedales, M. C. W. van Rossum, B. P. Graham and M. B. Dutia: Implications of noise and neural heterogeneity for vestibulo-ocular reflex fidelity, *Neural Comput.*, Vol. 20, No. 3, pp. 756-778, 2008.
- [9] A. Ochab-Marcinek, G. Schmid, I. Goychuk and P. Hänggi: Noise-assisted spike propagation in myelinated neurons, *Phys. Rev. E*, Vol. 79, No. 1, pp. 11904-11910, 2009.
- [10] S. A. Ibáñez, P. I. Fierens, R. P. J. Perazzo and D. F. Grosz: Performance robustness of a noise-assisted transmission line, *Physica D*, Vol. 238, No. 21, pp. 2138-2141, 2009.
- [11] T. Oya, I. N. Motoike and T. Asai: Single-electron circuits performing dendritic pattern formation with nature-inspired cellular automata, *Int. J. Bifurcation Chaos*, Vol. 17, No. 10, pp. 3651-3655, 2007.
- [12] A. Utagawa, T. Asai, T. Hirose and Y. Amemiya: An inhibitory neural-network circuit exhibiting noise shaping with subthreshold MOS neuron circuits, *IEICE Trans. Fundam.*, Vol. E90-A, No. 10, pp. 2108-2115, 2007.
- [13] A. Utagawa, T. Asai, T. Hirose and Y. Amemiya: Noise-induced synchronization among sub-RF CMOS analog oscillators for skew-free clock distribution, *IEICE Trans. Fundam.*, Vol. E91-A, No. 9, pp. 2475-2481, 2008.
- [14] A. K. Kikombo, A. Schmid, T. Asai, Y. Leblebici and Y. Amemiya: A bio-inspired image processor for edge detection with single-electron circuits, *J. Signal Proc.*, Vol. 13, No. 2, pp. 133-144, 2009.
- [15] A. K. Kikombo, T. Asai, T. Oya, A. Schmid, Y. Leblebici and Y. Amemiya: A neuromorphic single-electron circuit for noise-shaping pulse-density modulation, *Int. J. Nanotech. Mol. Comput.*, Vol. 1, No. 2, pp. 80-92, 2009.
- [16] A. K. Kikombo, T. Asai and Y. Amemiya: Neuromorphic circuit architectures employing temporal noises and device fluctuations to improve signal-to-noise ratio in a single-electron pulse-density modulator, *Int. J. Unconv. Comput.*, Vol. 7, Nos. 1-2, pp. 53-64, 2011.
- [17] A. Utagawa, T. Asai and Y. Amemiya: High-fidelity pulse density modulation in neuromorphic electric circuits utilizing natural heterogeneity, *Nonlinear Theory and Its Applications*, Vol. 2, No. 2, pp. 218-225, 2011.
- [18] N. Schweighofer, K. Doya, H. Fukai, J. V. Chiron, T. Furukawa and M. Kawato: Chaos may enhance information transmission in the inferior olive, *Proc. Natl. Acad. Sci. USA*, Vol. 101, No. 13, pp. 4655-4660, 2004.
- [19] G. M. Tovar, T. Asai and Y. Amemiya: Array-enhanced stochastic resonance in a network of noisy neuromorphic circuits, *Neural Information Processing: Theory and Algorithms*, *Lecture Notes in Computer Science*, Springer, Vol. 6443, pp. 188-195, 2010.
- [20] G. Nicolis, C. Nicolis and D. McKernan: Stochastic resonance in chaotic dynamics, *J. Stat. Phys.*, Vol. 70, Nos. 1-2, pp. 125-139, 1993.
- [21] E. Reibold, W. Just, J. Becker and H. Benner: Stochastic resonance in chaotic spin-wave dynamics, *Phys. Rev. Lett.*, Vol. 78, No. 16, pp. 3101-3104, 1997.
- [22] A. Kovaleva and E. Simiu: Chaotic resonance: hopping rates, spectra and signal-to-noise ratios, *Stochastic and Chaotic Dynamics in the Lakes*, D.S. Broomhead, E.A. Luchinskaya, P.V.E. McClintock and T. Mullin, Eds., American Institute of Physics, pp. 428-433, 2000.
- [23] L. Y. Chew, C. Ting and C. H. Lai: Chaotic resonance: two-state model with chaos-induced escape over potential barrier, *Phys. Rev. E*, Vol. 72, No. 3, pp. 36222-36234, 2005.
- [24] S. Nobukawa, H. Nishimura and N. Katada: Chaotic resonance by chaotic attractors merging in discrete cubic map and chaotic neural network, *IEICE Trans. A*, Vol. J95-A, No. 4, pp. 357-366, 2012.
- [25] I. Tokuda, C. E. Han, K. Aihara, M. Kawato and N. Schweighofer: The role of chaotic resonance in cerebellar learning, *Neural Networks*, Vol. 23, No. 7, pp. 836-842, 2010.

- [26] L. O. Chua, T. Matsumoto and M. Komuro: The double scroll, *IEEE Trans. Circuits Syst.*, Vol. 32, No. 8, pp. 798-818, 1985.
- [27] J. J. Collins, C. C. Chow and T. T. Imhoff: Stochastic resonance without tuning, *Nature*, Vol. 376, No. 20, pp. 236-238, 1995.

reconfigurable and parallel architectures and low-power circuits. He won the IEEE JSSC Annual Best Paper Award in 1992, the IPSJ Annual Best Paper Award in 1999, and the IEICE Achievement Award in 2011. He is a member of IEICE and IEEE.

(Received April 9, 2013; revised July 19, 2013)



**Kazuyoshi Ishimura** received his B.S. degree in electronic engineering from Tokyo Denki University, Japan, in 2010, and his M.S. degree in electrical engineering from Hokkaido University, Japan, in 2013. He is currently working toward his

Dr. Engineering degree in the Graduate School of Information Science and Technology, Hokkaido University, Sapporo, Japan. His research interests include nonlinear circuits and stochastic resonance.



**Tetsuya Asai** received his B.S. and M.S. degrees in electronic engineering from Tokai University, Japan, in 1993 and 1996, respectively, and his Ph.D. degree from Toyohashi University of Technology, Japan, in 1999. He is now an Associate Professor in the Graduate School of Information Science and Technology, Hokkaido University, Sapporo, Japan. His

research interests are focused on developing nature-inspired integrated circuits and their computational applications. Current topics that he is involved with include intelligent image sensors that incorporate biological visual systems or cellular automata in the chip, neurochips that implement neural elements (neurons, synapses, etc.) and neuromorphic networks, and reaction-diffusion chips that imitate vital chemical systems.



**Masato Motomura** received his B.S. and M.S. degrees in physics and his Ph.D. degree in electrical engineering in 1985, 1987, and 1996, respectively, all from Kyoto University. He was with NEC and NEC Electronics from 1987 to 2011, where he was engaged in the research and business development of dynamically reconfigurable processors and on-chip multicore processor architectures. He

moved to Hokkaido University in April 2011, where he is now a Professor in the Graduate School of Information Science and Technology. His current research interests include